Clim. Past, 21, 1661–1677, 2025
https://doi.org/10.5194/cp-21-1661-2025

Climate of the Past
Open Access
EGU

Edisto Inlet as a sentinel for Late Holocene environmental changes over the Ross Sea: insights from foraminifera turnover events

Giacomo Galli[1,2], Katrine Elnegaard Hansen[3], Caterina Morigi[2], Alessio Di Roberto[4], Federico Giglio[5], Patrizia Giordano[5], and Karen Gariboldi[2]

[1]Department of Environmental Sciences, Informatics and Statistics, Ca' Foscari University of Venice, Via Torino 155, 30172 Venice, Italy
[2]Department of Earth Sciences, University of Pisa, Via Santa Maria 53, 56126, Pisa, Italy
[3]Department of Near Surface Land and Marine Geology, The Geological Survey of Denmark and Greenland (GEUS), 8000 Aarhus C, Aarhus, Denmark
[4]National Institute of Geophysics and Volcanology (INGV), Via Cesare Battisti 53, 56125, Pisa, Italy
[5]National Institute of Polar Sciences (CNR-ISP), Via Piero Gobbetti 101, 40129, Bologna, Italy

Correspondence: Giacomo Galli (giacomo.galli@unive.it)

Received: 22 January 2025 – Discussion started: 7 February 2025
Revised: 15 July 2025 – Accepted: 16 July 2025 – Published: 23 September 2025

Abstract. Identifying marine environmental changes is important to understand the processes that govern the Earth's climate system and its interacting components. Microfossil assemblages are one of the most used palaeoenvironmental tracers, with their community composition responding to changes in the physiochemical characteristics of the environment. In this context, foraminifera have been extensively used due to their preservation potential. However, little attention has been paid to the properties of the whole foraminiferal community that, in turn, can be used to depict a comprehensive view of the environment. In this study we focused on the laminated marine sediment core TR17-08 collected in Edisto Inlet (Ross Sea, Antarctica) and the turnover events that characterized the benthic foraminiferal fauna over the last 3.6 kyr. Using rate-of-change (RoC) analysis, three distinct turnover events were recognized having a long-term effect on the fauna: at 2.7–2.5, 1.2–1.0 and 0.7 kyr BP. At 2.7–2.5 kyr BP, *Miliammina arenacea* disappears and are substituted by different calcareous species, such as *Epistominella exigua, Nonionella iridea* and *Stainforthia feylingi*. Aligning with the micropalaeontological interpretations, changes in X-ray fluorescence (XRF) ratios (Zr / Rb; Ca / Ti and Br / Ti) were coeval with the interpretation derived from the RoC and the microfossils assemblage composition. Over this transition, a switch from multi-year landfast sea ice (3.6–2.7 kyr BP) to a seasonal sea-ice-dominated environment (2.5–1.2 kyr BP) was driven by a change in the water mass characteristics, increasing the mCDW (modified Circumpolar Deep Water) content inside the fjord as well as increase the duration of the summer ice-free period. Higher RoC values suggested the absence of a stable benthic foraminifera community under the frequent multi-year landfast sea-ice scenario, while the lowest RoC values during the seasonal sea-ice phase are present, especially within the 2–1.5 kyr BP interval, aligning with the macrofaunal response inside the inlet. Continental archives (penguin and elephant seals remains) along the Victoria Land coast recorded such a change in the sea-ice type during the Late Holocene. This study provides further evidence of a change in the sea-ice state in the Ross Sea after 2.7–2.5 kyr BP, thus supporting that this water mass intrusion onto the continental shelf was more prominent during the 2.5–1.2 kyr BP period, in accordance with the persistent summer positive mode of the Southern Annular Mode. Lastly, this study highlights that using ecological properties of the benthic foraminifera community can be a valuable source of information for high-resolution studies and can provide additional insights into the palaeoenvironmen-

tal interpretation and palaeoclimatic reconstruction that uses benthic foraminiferal species as environmental indicators.

1 Introduction

Unveiling past environmental changes is fundamental to understanding the processes that governs the Earth's climate system, and it helps to pinpoint its behaviour in the future. To investigate the past environment, different proxies have been used to obtain a holistic view of all the interacting compartments of the climate system (Strugnell et al., 2022; Toyos et al., 2020; Wang et al., 2023; Wu et al., 2020; Yokoyama et al., 2016). In marine settings, a group that has been extensively used as a tracer for environmental changes are benthic and planktic foraminifera: unicellular marine eukaryotes, with different test material that have great preservation potential (Sen Gupta, 2003; Murray, 1991, 2006). These organisms inhabit both the surface and bottom water, and they can be used to infer changes in the palaeoenvironmental evolution of an area (Sen Gupta, 2003; Murray, 1991, 2006). However, most of the studies that have been carried out with foraminifera focus on comparing changes in the relative abundances of a single species or a group of species and connect them to specific changes in the environment (i.e., Ishman and Sperling, 2002; Kyrmanidou et al., 2018; Majewski et al., 2018).

Community-level (i.e., the whole assemblage considered one indivisible unit) analysis can help us understand the effects of different environmental phases on the local fauna, while also providing key insights into environmental evolution (Foster et al., 1990). However, little to no attention has been paid to the properties of the whole community that, potentially, can be used as a reliable tracer to identify significant turnover events linked to the succession of different environmental phases (Hansen et al., 2023; Tomašových and Kidwell, 2010).

In this context, the rate-of-change (RoC) analysis calculates the compositional changes in a given community through time to extrapolate the rate at which the whole community is changing. This can be used to infer statistically significant changes in the assemblage composition, the so-called turnover events (TEs) (Foster et al., 1990; Hansen et al., 2023; Jacobson and Grimm, 1986; Mottl et al., 2021b, a; Shimadzu et al., 2015). The analysis was used by Hansen et al. (2023) on the ecological traits of benthic foraminifera to infer ecological responses over the western coast of Greenland. This was crucial to understanding the consequences of the deglacial-Holocene and the mid-Holocene warming on the benthic foraminifera fauna in the area while simultaneously showing that TEs of benthic foraminifera can be linked to climatic perturbation.

In this study, we focus on the marine sediment core TR17-08 from Edisto Inlet (Ross Sea, Antarctica, Fig. 1) with the purpose of understanding short-term (centennial) and long-term (millennial) environmental changes in the area and how they connect with faunal turnover events.

Edisto Inlet is a small basin (16 km long, 4 km wide) located on the northern tip of Victoria Land in the Ross Sea, characterized by a 110 m thick laminated sedimentary sequence on the bottom, spanning the entire Holocene (Battaglia et al., 2024; Finocchiaro et al., 2005; Di Roberto et al., 2023; Tesi et al., 2020). Previous studies highlighted that environmental changes occurring in the inlet over the Late Holocene are linked to changes in the global climatic system, such as the Medieval Climate Anomaly (MCA, ca. 1.5–1.1 kyr BP) and the Little Ice Age (LIA, ca. 0.7–0.1 kyr BP) (Galli et al., 2023, 2024; Lüning et al., 2019; Mezgec et al., 2017; Stenni et al., 2017; Tesi et al., 2020). In addition, the study of Galli et al. (2024) on ophiuroid ossicles in conjunction with the diversity of the foraminiferal assemblage proposed a shift from an unstable seasonal sea-ice cycle (3.6–2.5 kyr BP) to a stable sea-ice cycle (2.5–1.5 kyr BP), with an optimum of these environmental conditions from 2 to 1.5 kyr BP. The latter has been regarded as the "Ophiuroid Optimum" because of the increase in the probability of occurrence of the ophiuroid *Ophionotus victoriae* and the lowest values of the $IPSO_{25}$ biomarker from the nearby marine sediment core HLF17-01 (Fig. 1c). This geochemical proxy is produced by diatoms that live inside the sea ice (sympagic), which are released upon the first break up of the sea ice (Belt et al., 2016). Due to the dependency of the sea-ice presence of sympagic diatoms to thrive, lower $IPSO_{25}$ concentrations have been connected to prolonged periods with an absence of a sea-ice cover (Belt et al., 2016; Massé et al., 2011; Tesi et al., 2020). The transition, occurring around 2.5 kyr BP, is characterized by a stepwise decrease in the flux and quantity of organic matter content, as testified by the reduction in the benthic and planktic foraminifera accumulation rates (BFAR and PFAR respectively) and by a decrease in the ice rafted debris (IRD) content that suggested the presence of seasonal sea-ice cover over this period (Galli et al., 2024).

In Edisto Inlet, the depositional regime is governed by the seasonal cycles of landfast sea ice, a particular type of sea ice that forms through the freezing of seawater and by remaining attached to the coast (Fraser et al., 2023). This seasonal behaviour produces the lamination pattern, which makes it related to the austral summer depositional setting. The first break up of the fjord sea-ice cover happens at the beginning of the austral spring season and leads to the deposition of a dark lamina (Tesi et al., 2020). This type of lamina is characterized by a diatom assemblage dominated by the *Fragilariopsis* genus. On the other hand, prolonged periods of ice-free scenarios lead to the deposition of a white laminae, which is dominated by the diatom *Corethron pennatum*, indicating an oligotrophication of the upper water column (Tesi et al., 2020). This is also reflected in the biomarker $IPSO_{25}$ (Belt et al., 2016). Since most of the depositional signal in the fjord is dominated by the summer season, if the previous interpreta-

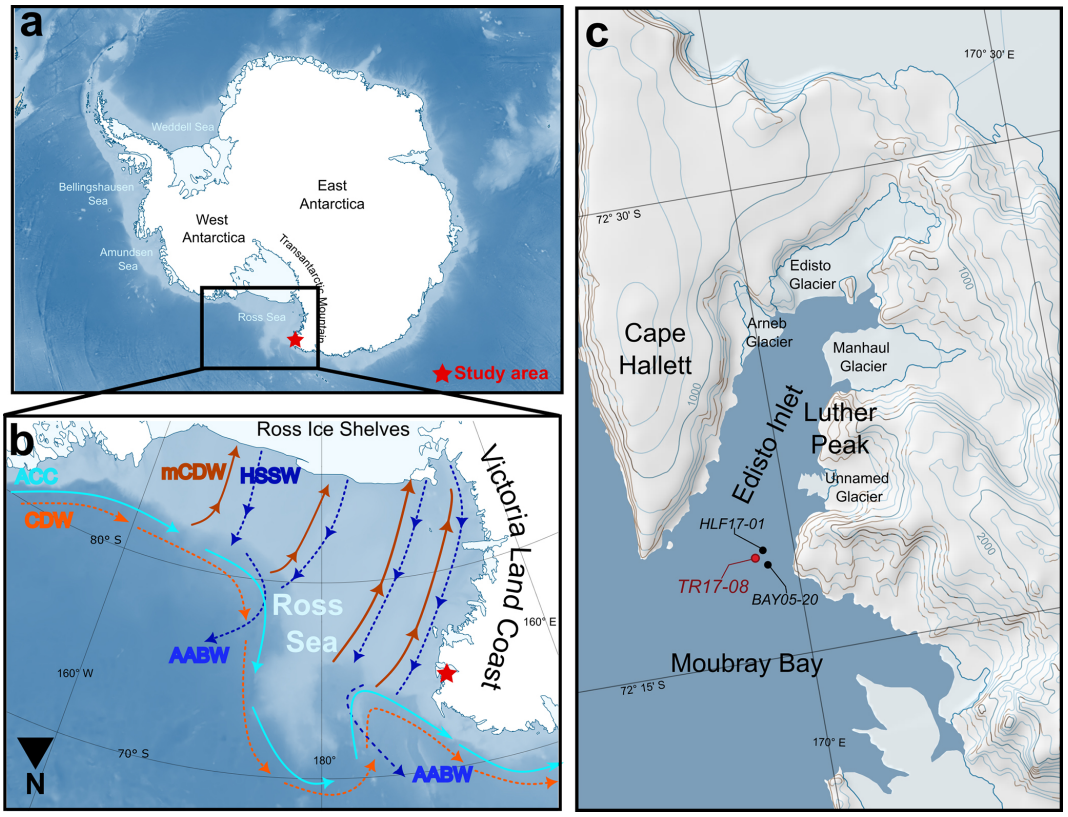

Figure 1. Simplified maps of the study area. **(a)** The location of the study area in Antarctica (red star). **(b)** Main oceanic currents: ASC: Antarctic Slope Current; CDW: Circumpolar Deep Water; mCDW: modified Circumpolar Deep Water; HSSW: High Salinity Shelf Water and AABW: Antarctic Bottom Water. Red colour arrows indicate relatively warm water masses while the blue colour ones indicate the relatively cold-water masses. Solid lines indicate surface water masses, while the dashed ones indicate deeper water masses. The star marks the location of Edisto Inlet. **(c)** Map of Edisto Inlet with analysed marine sediment cores mentioned in this study marked with dots: in red the marine sediment core TR17-08 (this study), while in black HLF17-01 (Tesi et al., 2020) and BAY05-20 (Mezgec et al., 2017). The maps are constructed using Quantarctica (Matsuoka et al., 2021).

tion of an unstable-to-stable transition occurred, then the rate at which the benthic community shifts should be higher before the transition, reflecting a period in which a stable community cannot form. In addition, we integrate the results of the RoC with X-ray fluorescence (XRF) data over the last 3.6 kyr, focusing on the 2.5 kyr BP transition to disentangle the environmental evolution of the area between these two different states.

Thus, the aim of this study is 2-fold: (1) connecting the presence of TEs with the presence of significant environmental shifts in the area and, by doing so, unlocking a new objective way of analysing benthic foraminiferal community and (2) reconstructing the palaeoenvironmental evolution over the 2.5 kyr BP transition to understand the relationship between local and regional changes over the study area.

Study area

The Ross Sea oceanographic circulation is density driven (Fig. 1b): the Antarctic Slope Current (ASC) sits on top of the warmer Circumpolar Deep Water (CDW), and they both flow westward along the slope. (Orsi and Wiederwohl, 2009; Smith et al., 2012; Whitworth and Orsi, 2006). The CDW can enter the continental shelf when it interacts with the saltier water masses that are flowing from the continent to the open ocean by reducing the inclination of the isopycnal (Fig. 1b; Budillon et al., 2011; Castagno et al., 2017; Smith et al., 2012). This modified water mass (modified Circumpolar Deep Water, mCDW) enters the continental shelf where it flows southwards, through bathymetric lows (Fig. 1b) (Dinniman et al., 2011; Wang et al., 2023). At the shelf, the inflow of the warmer water masses sustains large persistent ice-free areas, the polynyas (Mathiot et al., 2012; Rusciano et al., 2013). At this point the warm water mass loses its heat and subsides due to the increase in density by salt-rejection processes. As the sea-ice polynya form over the area, katabatic winds move the newly formed sea ice away from the continent, thus sustaining both the production of the sea ice, by cooling the sea surface, and the ice-free area (Dale et al., 2017; Drucker et al., 2011). This subsided water mass forms

the High Salinity Shelf Water (HSSW), which flows along the same bathymetric lows as the mCDW and arrives at the shelf margin, where it cascades onto the seafloor, forming the Antarctic Bottom Water (AABW) (Fig. 1b; Orsi and Wiederwohl, 2009; Wang et al., 2023; Whitworth and Orsi, 2006). Lastly, studying the current activity in the western part of the Ross Sea, it has been noted that the mCDW inflow is mostly seasonal and happens during the austral summer period (Castagno et al., 2017; Wang et al., 2023).

In particular, Edisto Inlet has an average water depth of 500 m, and the basin is defined by a sill at 400 m depth located at the mouth that divides it from the adjacent Moubray Bay (Fig. 1c). Four local marine-terminating glaciers are present: the Arneb Glacier, the Edisto Glacier, the Manhaul Glacier and an unnamed glacier located north of Luther Peak (Fig. 1c).

Oceanographic data and CTD profiles from the inner part of the fjord have shown the presence of a double layer stratification of the water column with a pycnocline/thermocline/halocline present at 50–150 m water depth (Battaglia et al., 2024). The surface layer is fresher and warmer than the deeper one ($< -1.8\,^{\circ}C$). Spatially, the surface waters are saltier (34.27 PSU) and colder ($-1.6\,^{\circ}C$) in the inner part of the fjord with respect to the outer ones (Battaglia et al., 2024).

In addition, the presence of sediment drifts at the bottom suggests the presence of relatively long-lived regular bottom water circulation starting at 8 kyr BP (Battaglia et al., 2024; Finocchiaro et al., 2005).

However, oceanographical data are scarce and for further and more detailed information about the geological and physical settings of the fjord, readers are referred to Battaglia et al. (2024).

2 Methods

To investigate the palaeoenvironmental evolution of the Edisto Inlet, the marine sediment core TR17-08 (72°18.2778′ S; 170°04.1784′ E; 462 m water depth) was retrieved during the XXXII PNRA (National Italian Program for Antarctic Research) scientific expedition (2016–2017) in the framework of the PNRA project TRACERS (PNRA16_00055). The core, with a length of about 14.5 m, is composed of diatomaceous ooze, with clear distinction between light and dark lamina (Galli et al., 2023; Fig. S1 in the Supplement). After a comprehensive reassessment of the age–depth model previously published by Di Roberto et al. (2023), we decided to employ the same model, given its robustness with respect to the application of different radiocarbon calibration curves and marine reservoir ages (More information in the Supplement). The bottom of the core was dated to around 3.6 kyr BP, with an average sedimentation rate of $0.5\,cm\,yr^{-1}$ from 3.6 to 0.7 kyr BP. Over the last 0.7 kyr, the sedimentation rate diminishes of an order of magnitude, with an average of $0.07\,cm\,yr^{-1}$ (Di Roberto et al., 2023). Foraminiferal assemblage data, benthic and planktic foraminifera accumulation rates (BFAR and PFAR respectively) and IRD (> 1 mm) fluxes were used in previous studies to analyse the environmental evolution of the last 2 kyr, as well as to the test the possibilities of using the macrofaunal remains to detect stable environmental conditions (Galli et al., 2023, 2024). Briefly, BFAR and PFAR have been extensively used to detect changes in the organic matter flux to the bottom and the primary productivity regime respectively (Herguera and Berger, 1991). The IRD flux has been associated with different glacial discharging regimes and with different sea-ice cover regimes, with lower values reflecting less glacial discharge and the presence of a prolonged ice-free regime (Christ et al., 2015; Reeh et al., 1999; Zhou et al., 2021). In this study, we extend the interpretation of the environmental evolution of this area using the micropalaeontological data collected by Galli et al. (2024).

2.1 Benthic foraminifera analysis

A TE can be defined as a drastic change in the species composition of a defined area (O'Sullivan et al., 2021; Shimadzu et al., 2015). Over extended periods, TEs can be linked to significant changes in environmental conditions, providing insights into the extent to which environmental shift can impact a given ecological community, in this case the benthic foraminifera (Foster et al., 1990; Hansen et al., 2023; Mottl et al., 2021b, a). To assess how the evolution of the environment was affecting the benthic foraminiferal community, we computed and analysed the rate-of-change (RoC) curve derived from the changes in relative abundances of the benthic species.

RoC analysis is a statistical method that computes the significance of a turnover events (TEs) in a palaeoecological temporal series in relation to the rate at which the community is changing (Hansen et al., 2023; Jacobson and Grimm, 1986; Mottl et al., 2021b). The analysis is based on the concept of calculating the differences between adjacent stratigraphic levels (beta diversity) to identify the times of significant shifts in the biological community (Mottl et al., 2021b, a). These significant changes in time can be detected with several methods: with a linear trend, a nonlinear trend, the first derivative of the curve or a signal-to-noise ratio (Mottl et al., 2021b). In our study we compare significant peaks detected by the nonlinear trend method (recommended for palaeoecological temporal series) and the significant departure from 0 of the first derivative of the curve (Mottl et al., 2021). The first of the chosen method identifies significant compositional changes as points exceeding a 1.5 standard deviation threshold derived from a fitted non-linear trend (TnL). The second method is based on the first derivative of a fitted generative additive model (GAM derivative method, Gd). The Gd detects a cluster of points when the first derivative of a

fitted GAM of the RoC curve is significantly below 0, and it can be used to represent the outcome of a TE (Mottl et al., 2021b, a; Simpson, 2018). These two detection methods can be used to infer significant TEs in a robust way since TnL and Gd are complementary with respect to what they detect (Fig. 2).

The RoC analysis was performed using the *R-Ratepool* package in R using a randomization factor of 10 000, with the recommended setup described in Mottl et al. (2021b). To account for the temporal resolution, we changed the "time standardisation" parameter to 100 and the window was set to 5 to have a similar resolution between the analysis and the sample step of the core (RoC analysis is performed every 20 years). To create the bins used to calculate the differences in the assemblages, we used the "binning with a moving window" approach as described and recommended in Mottl et al. (2021b). To better display the trends of the RoC curve a GAM model (algorithm: REML) was fitted using the *mgcv* package (Simpson, 2018; Wood, 2001).

In addition to analysing the whole period, we also performed analysis on the 3.6–0.7 kyr BP period, due to the presence of a substantial change in the sedimentation rate (Galli et al., 2023; Di Roberto et al., 2023).

2.2 Sediment properties and lithology

To reconstruct the changes in the sedimentary depositional environment of the study area, a third-generation AVAATECH core scanner was used to acquire high-resolution XRF data at 1 cm intervals at the Institute of Marine Sciences at the Italian National Research Council (CNR-ISMAR) of Bologna. The base-10 logarithm of Zr / Rb, Br / Ti and Ca / Ti was used to interpret sedimentary, environmental and climatic processes as suggested by Croudace and Rothwell (2015). These ratios have been extensively used in palaeoenvironmental reconstruction. The Zr / Rb ratio has been used to track changes in the mean grain size of the silt fraction that can be linked to current strength, with high values reflecting a high-current dynamic (Lamy et al., 2024; Wu et al., 2019, 2020). The Br / Ti ratio can be used to infer changes in the primary productivity, since Br is related to organic matter of marine origin (Wu et al., 2019; Ziegler et al., 2008), while the Ca / Ti ratio has been used to infer changing in the biogenic vs. lithogenic sedimentation due to the more prominent presence of Ti in the detrital material and Ca mostly derived from biogenic mineralization (Piva et al., 2008; Taylor et al., 2022). To reduce the noise of these temporal series, a LOESS smoothing curve with a narrow smoothing window ($\lambda = 0.1$) was fitted using the function *lm* of the base version of R (R Core Team, 2023).

3 Results and discussion

3.1 Turnover events over the last 3.6 kyr in Edisto Inlet

Turnover events (TEs) were defined only over the benthic foraminiferal community due to the presence of only one planktic species: *Neogloboquadrina pachyderma* (Galli et al., 2024).

The RoC computed for the species composition shows the presence of Gd clusters starting at 3.3, 2.5 and 0.7 kyr BP (Fig. 3a). Of these three Gd clusters, only the latter has significant points of both TnL and Gd, reflecting a large environmental shift, as inferred by the foraminiferal assemblage (1.1–0.6 kyr BP). This can also be inferred by the increase in the RoC at its maximum values (> 0.8, Fig. 3a).

When taking into consideration only the 3.6–0.7 kyr BP period, a cluster of TnL peaks is present at 3.2–3 kyr BP, at 2.7–2.5 kyr BP, at 1.2–1 kyr BP, and a single point at 0.7 kyr BP (Fig. 3b). The 3.2–3 kyr BP event is coincident with the presence of a Gd cluster at 3.3–3 kyr BP (Fig. 3a). Over the 3.6–2.7 kyr BP period, both RoC curves show no distinctive trend, thus indicating no significant increase or decrease in the compositional change in the benthic foraminiferal community after the 3.3–3 kyr BP event (Fig. 3). At 2.7–2.5 kyr BP, TnL points are followed by Gd points (Fig. 3b), with the latter appearing in both analyses (Fig. 3). In contrast to 3.3–3 kyr BP, the presence of a visible downward trend of the RoC curves after 2.5 kyr BP suggests that this event was caused by an environmental shift that had a long-term effect on the fauna (Fig. 3b). The downward trend lasted until 1.8 kyr BP, while similar values of the RoC analysis from the 3.6–2.7 kyr BP period are found at 1.5 kyr BP (Fig. 3b). A presence of a steeper increase starting at 1.5 kyr BP is also visible in the RoC evaluated over the whole period (Fig. 3a).

Afterwards, several TnL from 1.2 to 1 kyr BP without being followed by Gd clusters are present, and a peak at 0.7 kyr BP is reached (Fig. 3). Both the 1.2–1 and the 0.7 kyr BP points are present over an upward trend (Fig. 3b). Thus, a period that is characterized by a high degree of instability, which can probably be inferred as reflecting a transitional period (Mottl et al., 2021a). Hence, the period 1.2–1 kyr BP is connected to a different TE than the one at 0.7 kyr BP because of the segregation of the TnL clusters (Fig. 3b). The most recent TnL point (Fig. 3b) is probably caused by substantial environmental shifts occurring at 0.7 kyr BP. This is highlighted in the RoC computed throughout the whole period, reflected by the presence of both TnL and Gd peaks, as well as by reaching the maximum RoC value at that time (Fig. 3a).

The last 2 kyr were previously investigated for benthic association, and a succession of different environmental phases was hypothesized (Galli et al., 2023). Over this period, the benthic foraminiferal assemblages were indicative of a seasonal sea-ice phase of the fjord (2–1.5 kyr BP) followed by a

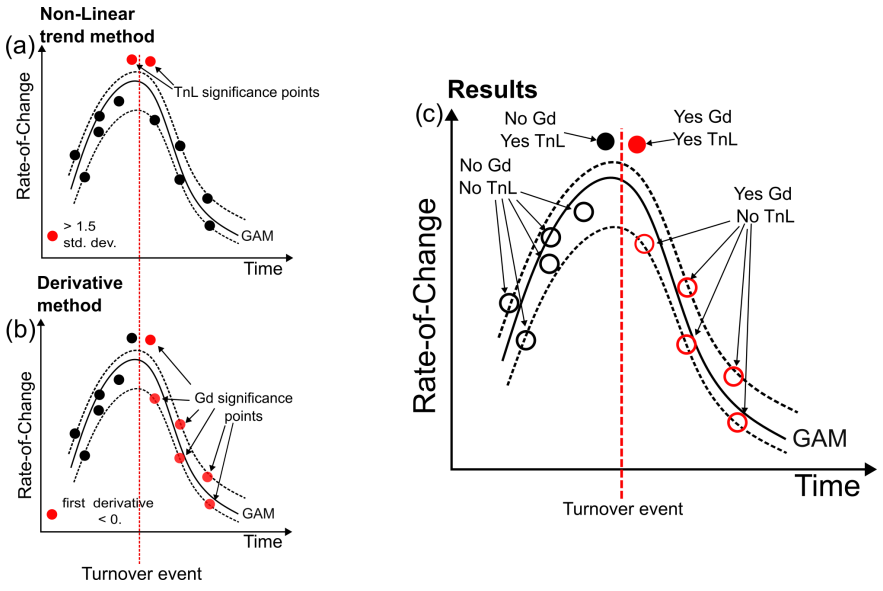

Figure 2. Schematic version of the rate-of-change (RoC) analysis used in this study to analyse the environmental impact on the foraminiferal community. **(a)** Non-linear trend detection method (TnL) that relies on points > 1.5 SD of a fitted non-linear trend. **(b)** GAM derivative method (Gd) that relies on the first derivative being < 0. **(c)** End results of the analysis when the significant TnL and Gd points are combined. In this conceptual example, the turnover event (dotted red line) is represented as an instantaneous event.

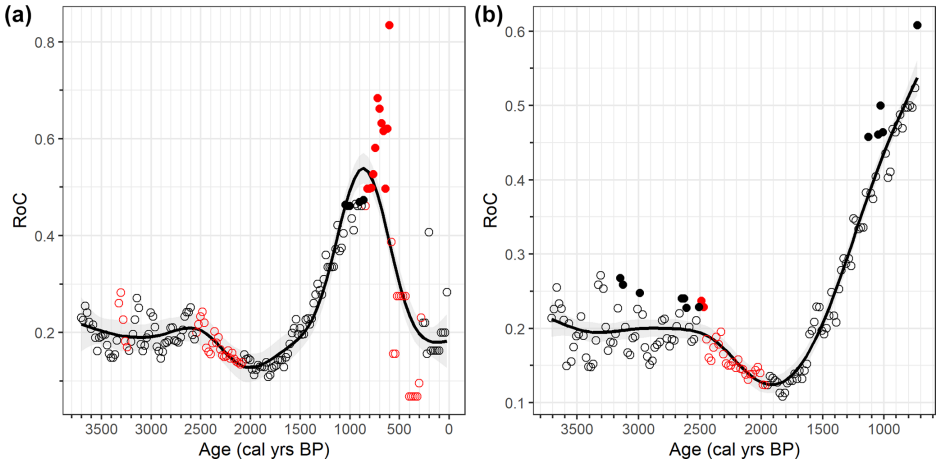

Figure 3. Results from RoC analysis of the benthic foraminiferal species. **(a)** Results for the whole core; **(b)** results of the analysis evaluated over 3.6–0.7 kyr BP. Red colours indicate significant Gd points, while black indicates the opposite. Filled circles indicates the significant TnL points. For further information the reader is referred to Sect. 3.

transitional phase (1.5–0.7 kyr BP) while the last 0.7 kyr are indicative of a cold and almost completely sea-ice-covered fjord causing a sharp reduction in the sediment accumulation rate by an order of magnitude (Di Roberto et al., 2023; Tesi et al., 2020). Moreover, the transitional phase of the fjord culminated with a complete switch from calcareous-dominated fauna to agglutinated-dominated at 1.1 kyr BP (Galli et al., 2023; Fig. 4). This transition of the dominant test material, coeval with a regional reduction of 2 °C over the Victoria Land region (Stenni et al., 2017). In this context, the RoC analysis agrees with this environmental evolution: lower values of the RoC over the 2–1.5 kyr BP period are followed by a steeper increase in the compositional changes over 1.5–0.7 kyr BP (Fig. 3a). During the period of increased instability of the community (increase in the RoC values), the presence of TnL at 1.2–1 kyr BP is coeval with the switch in the dominant component of the fauna (Fig. 4): during the 2–1.5 kyr BP interval, the fjord transitions from a seasonal sea-ice phase to a completely covered fjord after 1.1 kyr BP (Galli et al., 2023). Thus, the RoC curve aligns with the evolution of the sea-ice cover duration, with higher ecological

instability increasing throughout the last 2 kyr caused by the reduction in the ice-free period.

Following these interpretations, the presence of a difference in the average values of the RoC between 3.6–2.7 and 2.5–1.5 kyr BP might be indicative of a switch of the state of the sea-ice cover during the summer, from a short ice-free period to a completely ice-free one at 2.7–2.5 kyr BP. Moreover, the presence of TnL at 3.3–3 kyr BP is indicative of this ecological instability over the 3.6–2.7 kyr BP period. On the other hand, lower RoC values and a clear downward trend over the 2.5–1.8 kyr BP period suggests a higher ecological stability associated with increasing ice-free conditions over the summer.

The benthic foraminiferal species reflect this change in the system state. Throughout the 3.6–1.5 kyr BP period, the fauna is dominated by calcareous species such as *Globocassidulina biora* and *Globocassidulina subglobosa* (> 50 % of the total assemblage, Fig. 4). These two common species have been found in Antarctic fjords and sub-ice shelf environments and have been used as indicator species for high hydrodynamic activities of the bottom water as well as high input of seasonal organic matter to the sea bottom (Bernhard, 1993; Harloff and Mackensen, 1997; Ishman and Szymcek, 2003; Kyrmanidou et al., 2018; Li et al., 2000; Majewski, 2023; Majewski et al., 2016, 2018; Melis et al., 2021; Sabbatini et al., 2004). In Admiralty Bay (King George Island, Antarctica) specimens belonging to the *Globocassidulina* group are the dominant species of the fjord-like environment, even below 400 m water depth, with dead assemblages dominated by *G. biora* specimens (Majewski, 2005, 2010). Hence, the dominance of *G. biora* from the TR17-08 record implies the presence of a fjord-like environment. Agglutinated species such as *Paratrochammina bartrami* and *Portatrochammina antarctica* are also reported as being constituent of fjord-like environments, especially at the > 400 m water depth (Majewski, 2005, 2010). This is also reflected in the TR17-08 record, with both species having low values of relative abundances (< 20 %) with isolated peaks from 3.6 to 1.5 kyr BP, paralleling the interpretation derived from *G. biora* and *G. subglobosa* (Fig. 4).

At 3.1 kyr BP (> 20 %) a peak in the relative abundance of the species *Nonionella iridea* is present (Fig. 4). This species is known to prefer environments that are rich in organic matter and with steep oxygen gradients inside the sediments (Fig. 4, Duffield et al., 2015). Thus, the abrupt increase in *N. iridea* might derive from the presence of a substantial quantity of organic matter arriving at the bottom, probably linked to an algal bloom in the surface layer. However, this event had no long-term effect on the benthic assemblage composition as suggested by the RoC curve (Fig. 3), reflecting an anomaly from the natural environment behaviour rather than a systematic change.

The TE occurring at 2.7–2.5 kyr BP is reflected by the changes in the distribution of the calcareous species *Epistominella exigua, Stainforthia feylingi* and *Trifarina angulosa* along with the almost disappearance of the agglutinated species *Miliammina arenacea* and a sudden increase in the *Portatrochammina antarctica* (Fig. 4).

The agglutinated miliolid *M. arenacea* thrives in environments with highly corrosive conditions at the bottom and/or where cold and salty water masses are present (Ishman and Szymcek, 2003; Li et al., 2000; Majewski et al., 2018; Murray, 1991). From 3.6 to 2.7 kyr BP the relative abundance of this species is relatively constant through time (Fig. 4). However, the period following the TE (2.5–1.5 kyr BP) is characterized by the almost complete disappearance of this species (Fig. 4). This change cannot be ascribed to an increase in the corrosive conditions as carbonate remains the dominant test material throughout the 3.6–1.5 kyr BP interval (Fig. 4). Thus, the disappearance of *M. arenacea* at 2.7 kyr BP must be associated with a change in the water masses characteristics.

Even in low percentages, the presence of *E. exigua* in relative higher values during and after the TE can be indicative of the presence of a warmer water mass, such as the mCDW in the fjord, and the presence of phytodetritus input from the surface layer (Fig. 5, Harloff and Mackensen, 1997; Ishman and Szymcek, 2003; Majewski et al., 2018; Sabbatini et al., 2004). The more continuous presence of high organic matter indicator species such as *N. iridea* and *S. feylingi* also suggests an increased flux of organic matter to the bottom (Duffield et al., 2015; Knudsen et al., 2008; Seidenkrantz, 2013; Seidenstein et al., 2018). The overall increase in these species can be caused by the presence of more frequent and prolonged ice-free conditions, having the effect of increasing the organic matter delivery to the bottom over the ice-free period, aligning with the RoC curve (Bart et al., 2018; Majewski and Anderson, 2009; Murray and Pudsey, 2004; Tesi et al., 2020). This is further supported by the sharp increase in *Portatrochammina antarctica*, an agglutinated species sensitive to increases in primary production (Majewski et al., 2020).

Moreover, species such as *Trifarina angulosa* have been used as an indicator of a high energy environment at the bottom, reflecting the presence of bottom water circulation (Ishman and Szymcek, 2003; Melis and Salvi, 2009). Despite being low in percentage, the presence is homogeneous throughout the 3.6–1.5 kyr BP period, except during the 2.7–2.5 kyr BP interval (Fig. 4), reflecting a decrease in the strength of the circulation over this time.

Hence, over the 3.6–1.5 kyr BP interval, from 3.6 to 2.7 kyr BP, the fjord is characterized by cold and salty bottom water conditions, a bottom water circulation and less primary productivity, with higher RoC values indicating less ice-free conditions over the summer season. At 2.7–2.5 kyr BP the transition occurs, with the disappearance of *T. angulosa* suggesting a shutting down of the bottom water circulation. From 2.5 to 1.5 kyr BP, the benthic fauna suggests more intrusions of mCDW, an increase in both primary productivity and organic matter flux to the sea floor (Fig. 4). The RoC

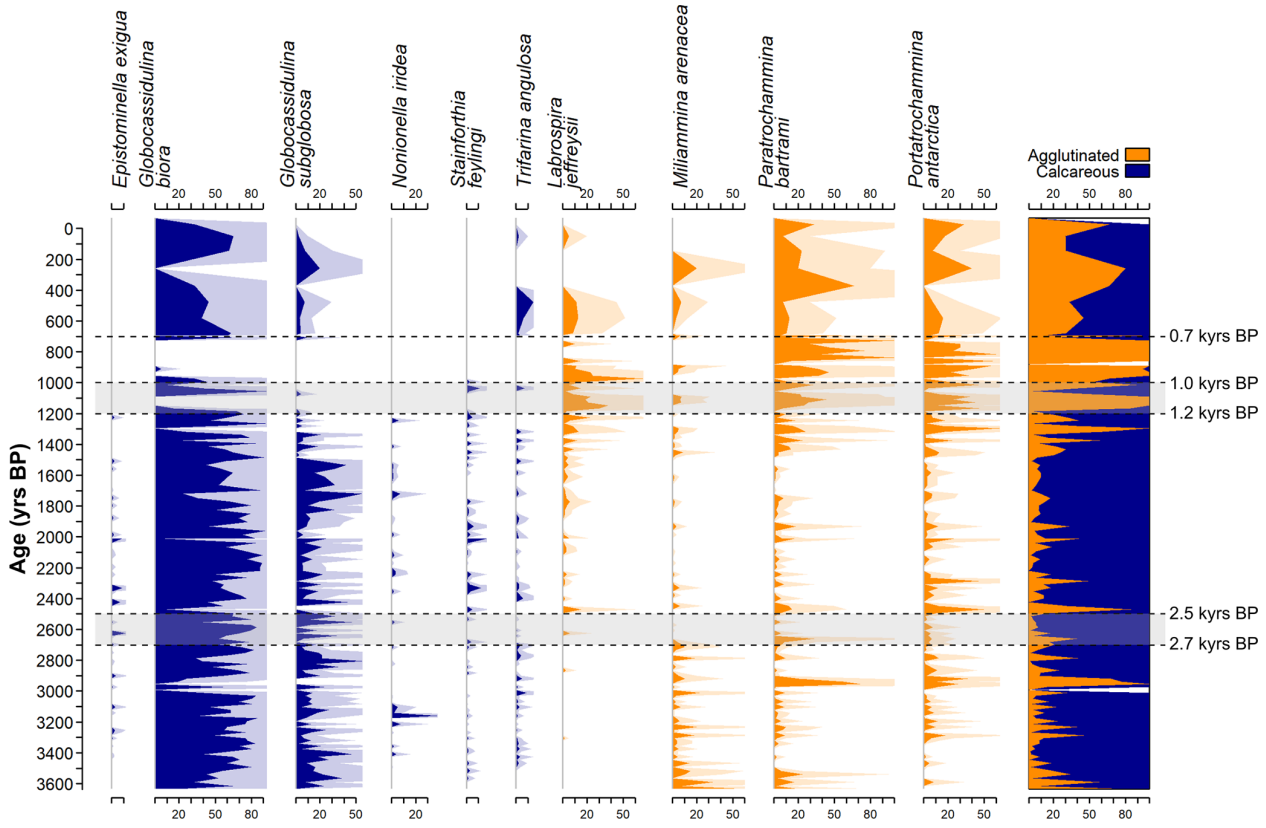

Figure 4. Benthic foraminifera relative abundances of common species (> 10 %) over the last 3.6 kyr, divided as calcareous (blue) and agglutinated species (orange). Dashed black lines and grey areas represent temporal locations of the turnover event as defined by the RoC analysis (see text for further details). On the last panel on the right, the white areas represent barren samples. Shaded areas represent exaggerated silhouettes (×4) to enhance the visibility of less common species. All plots have the same scaling of the *x* axis with one tick indicating 10 % relative abundance.

values over this period suggest the presence of a prolonged period of ice-free conditions over summer.

3.2 Environmental transition at 2.7–2.5 kyr BP

To have a comprehensive outlook of the environmental transition that characterized Edisto Inlet around 2.7–2.5 kyr BP, the RoC curves (Fig. 3) and the benthic assemblages (Fig. 4) were compared with the geochemical proxies derived from the TR17-08 sediment core, as well as previously published records from the same core and others derived from nearby marine sediments cores (Fig. 1c, HLF17-01 and Bay05-20c) (Galli et al., 2023, 2024; Mezgec et al., 2017; Tesi et al., 2020). A summary of the interpretations is reported in Table 1.

Over 3.6–2.7 kyr BP, higher RoC values occur along with the low probability of occurrence of the ophiuroid *Ophionotus victoriae* (P(O), Fig. 5a). Lower values of the P(O) can be associated with unstable seasonal sea-ice conditions due to the dependency of this organism on stable interannual conditions (Fig. 5a, Galli et al., 2024). The benthic foraminiferal assemblage suggests the presence of bottom currents, cold and salty bottom water conditions and low productivity (Fig. 5a). The presence of bottom currents is also suggested by the stable values of the Zr / Rb ratio (Fig. 5b), while the low values of both Ca / Ti and Br / Ti are indicative of low primary productivity (Fig. 5c). However, in Galli et al. (2024) the high variability in the BFAR and PFAR has been associated with an increase in the organic matter flux to the sea floor with the presence of abrupt increases in primary productivity (Fig. 5d and e), also suggested by the peak of *Nonionella iridea* at 3.1 kyr BP (Fig. 4). The presence of prolonged periods with multi-year landfast sea ice could explain these apparent discrepancies between the geochemical and micropalaeontological proxy. The present-day setting of Edisto Inlet is mainly controlled by the presence of seasonal landfast sea ice (Battaglia et al., 2024; Tesi et al., 2020). Landfast sea ice is prone to becoming multi-year and can show high nutrient concentrations, since it can be stored and accumulate on the basal portion of sea ice for multiple consecutive years. This could lead to an increase in sea-ice-associated diatoms, hence resulting in an abrupt increase in the organic matter flux to the bottom upon first break-up (termed “high nutrient high chlorophyll paradox”;

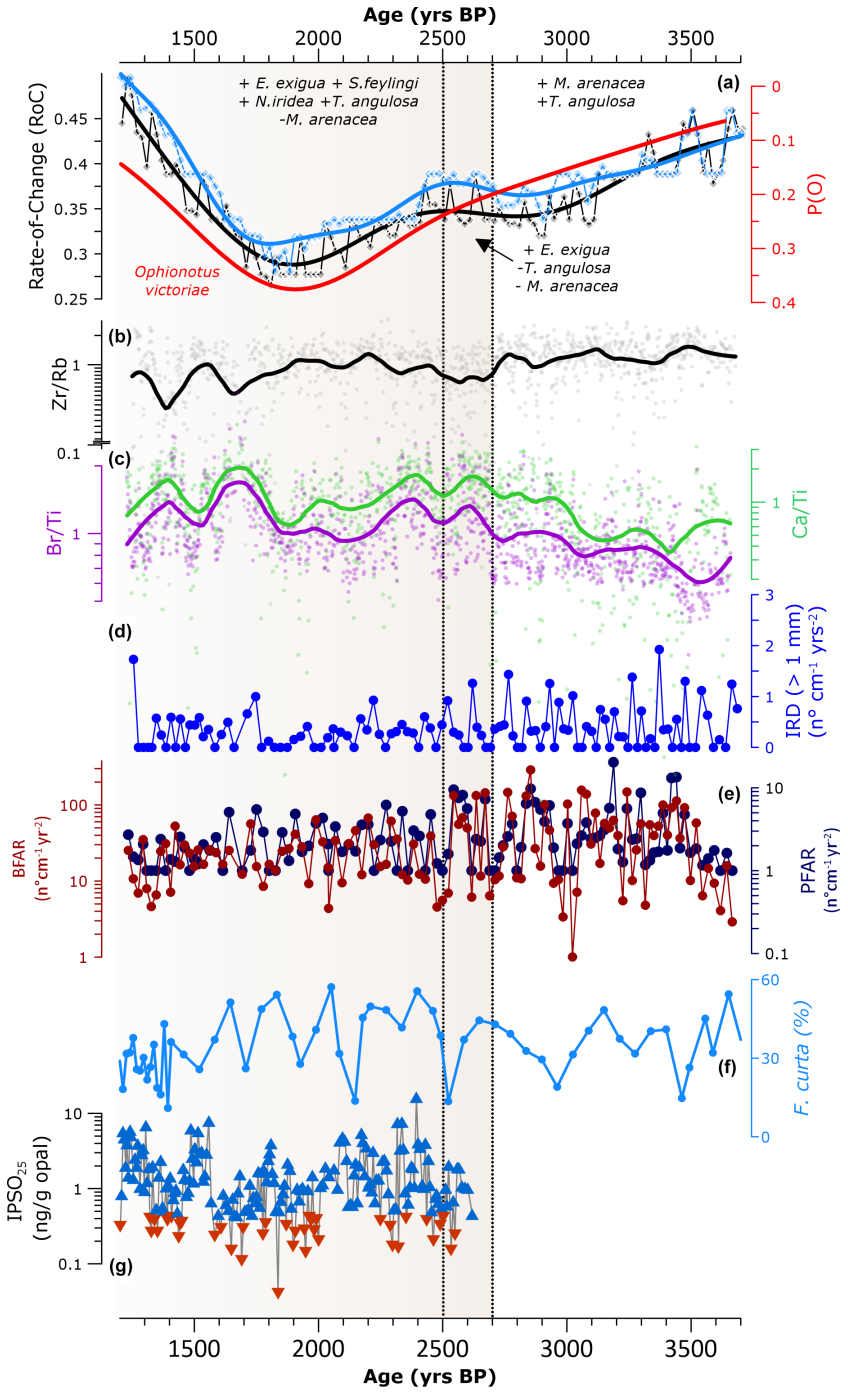

Figure 5. Palaeoenvironmental evolution from 3.6 to 1.5 kyr BP in Edisto Inlet. Different background colours are used to highlight the transition from a multi-year sea-ice environment to a seasonal sea-ice one. Vertical dotted black lines are indicative of the turnover events (TEs) at 2.7–2.5 kyr BP. **(a)** Rate-of-change (RoC) results (points) and fitted GAM models (line) throughout the core (in black) and for the 0.7–3.6 kyr BP period (in light blue). The red line indicates *Ophionotus victoriae* presence modelled as the probability of occurrence using a GAM model (P(O), from Galli et al., 2024). The names indicate the difference benthic foraminiferal species discussed in Sect. 3.1 with + symbol indicating higher abundances and – symbol indicating less presence. **(b)** Logarithm in base 10 of the ratio Zr / Rb (grey dots refer to raw data, the black line represents the fitted LOESS); **(c)** Primary productivity indicators: Ca / Ti (green) and Br / Ti (purple); **(d)** ice-rafted debris flux (IRD, blue, from Galli et al., 2024). **(e)** Benthic foraminifera accumulation rate (BFAR, brown) and planktic foraminifera accumulation rate (PFAR, dark blue, from Galli et al., 2024). The logarithm in base 10 was applied to enhance the visibility of the variability in the fluxes values; **(f)** *Fragilariopsis curta* relative abundance from the core BAY05-20 (from Mezgec et al., 2017). **(g)** $IPSO_{25}$ values in logarithm in base 10 from the HLF17-01 with blue and red triangles indicating different summer sea-ice cover: red indicates ice-free summer, blue the presence of summer sea-ice cover (threshold values from Tesi et al., 2020).

Table 1. Summary of Edisto Inlet proxy and environmental succession over 3.6–1.5 kyr BP. Associated with the climatic phase in kyr BP, a qualitative description of the TR17-08 proxy behaviour (↑ is relatively high, ↓ is relatively low, – is no change), the characteristic benthic foraminiferal species and the schematic environmental phase description are provided. For further detail the readers are referred to Sect. 3.2 of this article.

Interval (kyr BP)	Indicators	Species Presence	Interpretation
3.6–27	↑ IRD; BFAR; PFAR; Zr / Rb; P(O); RoC. ↓ *F. curta*; Ca / Ti; Br / Ti.	↑ *M. arenacea* and *T. angulosa* ↓ *E. exigua*, *N. iridea, S. feylingi*	cold and salty bottom water; multi-year sea-ice cover; occurrence of abrupt increases in primary productivity
2.7–2.5	↑ P(O); Br / Ti; Ca / Ti; RoC. ↓ IRD; Zr / Rb; BFAR; PFAR.	↑ *E.exigua* ↓ *M. arenacea* and *T. angulosa*	transitional event: intrusion of mCDW and increase in glacier run-off
2.5–1.5	↑ P(O); Zr / Rb; Br / Ti; Ca / Ti. – IRD; BFAR; PFAR. ↓ RoC; $IPSO_{25}$.	↑ *E.exigua*; *N. iridea, S. feylingi* and *T. angulosa* ↓ *M. arenacea*	seasonal sea-ice phase with the presence of mCDW and high primary productivity

Fraser et al., 2023; Wongpan et al., 2024). Thus, while surface productivity can be high over a short time frame due to the presence of algal blooms, as indicated by the BFAR and PFAR values, this might not have any effect on a longer time frame, as shown in the Br / Ti and Ca / Ti ratios, because of the prolonged ice cover (Fig. 5c). In addition, low percentages of *Fragilariopsis curta* from the nearby Bay05-20 sediment core also support this interpretation, since without the presence of a seasonal sea-ice regime, this diatom cannot thrive, explaining the relatively low values with respect to the subsequent phase (Fig. 5f) (Leventer et al., 1993; Mezgec et al., 2017; Waters et al., 2000).

At 2.7–2.5 kyr BP the TE in the benthic foraminifera highlights the transition from a cold and salty bottom water and low productivity setting to a state in which intrusion of mCDW along with a high primary productivity are present, as suggested by the higher abundance of *E. exigua* and the absence of *M. arenacea* (Fig. 5a). In addition, the absence of *T. angulosa* suggests the absence of a bottom current circulation over this short time interval (Fig. 5a).

These changes in the benthic foraminiferal composition occur in conjunction with a sudden reduction in the Zr / Rb values (Fig. 5b), and a peak in both the Br / Ti and Ca / Ti ratios, aligning with the benthic foraminifera interpretation (Fig. 5c).

The increase in the primary productivity along with the change in the circulation strength might be related to an increase in the meltwater derived from the marine-terminating glaciers. Glacial meltwaters in enclosed basins have the effect of enhancing the mixing of the water column, increasing the nutrient content available in the surface layers (Howe et al., 2010; Pan et al., 2020). However, if the increase in the meltwater content exceeds a certain value, the presence of fresh water can reduce and even shut down the estuarine circulation (Pan et al., 2020).

After the 2.7–2.5 kyr BP event, the benthic foraminiferal RoC reaches the lowest values, reflecting an increasing stability of the summer season (Fig. 5a). This aligns with the macrofaunal response: the P(O) increases to its maximum values, suggesting a stable interannual seasonal sea-ice cycle (Galli et al., 2024). The Zr / Rb ratio is increasing from 2.5 to 1.8 kyr BP (Fig. 5b), suggesting a slow restoration of the thermohaline circulation inside the fjord in accordance with the frequent presence of *T. angulosa* (Fig. 4). Both Ca / Ti and Br / Ti identify a period characterized by a higher average values with respect to 3.6–2.7 kyr BP, suggesting an increase in the primary productivity as well as in the organic matter flux to the bottom, consistent with more frequent presence of *N. iridea* and *S. feylingi*, as well as an increase in the *Epistominella exigua* content (Fig. 5a). This species became more frequent over the 2.5–1.5 kyr BP interval, suggesting an increase in the mCDW intrusion inside the inlet (Fig. 4). Intrusion of this warm and nutrient-rich water mass can cause an increase in primary productivity as well as stabilizing summer conditions, promoting prolonged ice-free austral summer (Dinniman et al., 2011; Dale et al., 2017). This aligns with the BFAR and the PFAR record that suggest a more stable input of organic matter with respect to the previous phase (Fig. 5d, Galli et al., 2024). Moreover, the relatively low content of IRD is indicative of prolonged ice-free conditions over the summer season, implying the presence of a seasonal sea-ice cover (Fig. 5d) (Christ et al., 2015; Galli et al., 2024; Peck et al., 2015). In addition, the *Fragilariopsis curta* in core Bay05-20 increases its relative abundances over this period, strengthening the hypothesis of a seasonal sea-ice regime (Allen and Weich, 2022; Leventer et al., 1993; Waters et al., 2000) (Fig. 5f).

Moreover, the period from 2 to 1.5 kyr BP has been proposed to be the most "stable" with respect to the seasonal sea-ice phase of the fjord due to high P(O) and lowest $IPSO_{25}$ values (Fig. 5a–g, Galli et al., 2024). This is supported by the presence of lowest RoC values, indicating the presence of a prolonged ice-free period, promoting benthic community stability.

3.3 Edisto Inlet as a sentinel for ocean dynamics in the western Ross Sea over the Late Holocene

Over the Victoria Land coast, and in general over the Ross Sea, different proxies refer to a similar period as the environmental transition occurring in Edisto Inlet regarding sea-ice conditions. Hall et al. (2023), studying the distribution of the southern elephant seals (*Mirounga leonina*) remains over the mid- and Late Holocene, inferred an increase in open water conditions as well as a reduction in the sea-ice presence from 2.3 to 1.8 kyr BP. They ascribed this ecological dynamic to an increase in the modified mCDW intrusion over Victoria Land, having a strong negative effect on the local marine-terminating glacier (Hall et al., 2006, 2023).

Another tracer of mCDW intrusion over the Ross Sea is the presence of Adelie penguin (*Pygoscelis adeliae*) colonies (Hall et al., 2023; Xu et al., 2021). Adelie penguins occupy a different ecological niche than elephant seals despite both relying on the presence of an ice-free zone to feed (Emslie et al., 2003, 2018; Hall et al., 2006). Since penguins rely on the presence of a consolidated ice platform to breed, while elephant seals do not, due to the increased number of penguins colonies ("Penguin Optimum", 4.6–2.8 kyr) followed by an increased number of southern elephant seal colonies ("Southern Elephant Seal Optimum", 2.3–1.8 kyr BP), Hall et al. (2023) inferred that over 5–2.7 kyr BP, the coastal Victoria Land region was a landfast-ice-dominated environment, while, from 2.5 to 0.5 kyr BP, a period of warmer-than-present climate occurred that may be related to a strengthening of the mCDW intrusion. The 2.5–0.5 kyr BP interval is also associated with prolonged ice-free conditions.

The switch in the sea-ice conditions over the Victoria Land region is coeval with the TE occurring in the benthic foraminifera community at 2.7–2.5 kyr BP (Hall et al., 2023). This local transition might be linked to an increased regional intrusion of mCDW over the western coast of the Ross Sea (Fig. 6). An addition to the overall content of mCDW could (1) sustain the ice-free period; (2) increase the glacial input derived from the melting of the marine-terminating glacier and (3) enhance the primary productivity, due to the high nutrient concentration that this water mass has (Arrigo and van Dijken, 2004; Dale et al., 2017; Dinniman et al., 2011; Emslie et al., 2003; Hall et al., 2006; Mathiot et al., 2012; Orsi and Wiederwohl, 2009; Smith et al., 2012; Smith and Gordon, 1997; Wang et al., 2023; Xu et al., 2021). Over the transition period, the intensification of glacier run-off would have promoted the thawing of the marine-terminating glaciers and increased the meltwater content. This has the effect of reducing the circulation inside the inlet, thus implying a stronger influence of the mCDW over the study area.

In addition, the presence of mCDW inside the inlet is reasonable due to the bathymetric distribution that this water mass has over the Ross Sea region. The mCDW is generally found at depth of around 200–400 m and, within the Drygalski Trough, this water mass flows southward, being consistent with the morphological features that characterized the inlet (Castagno et al., 2017; Orsi and Wiederwohl, 2009; Smith et al., 2014; Wang et al., 2023; Zhang et al., 2024). Since this should be a regional response, another key element is the presence of a relation between the upwelling of CDW onto the continental shelf and a positive phase of the Southern Annular Mode (SAM, Fig. 6c). The SAM is defined as a latitudinal gradient of sea-level pressure between middle and high latitudes (Fogt and Marshall, 2020; Marshall, 2003). Positive phases of this atmospheric mode are associated with the strengthening and the poleward movement of the westerlies that, in turn, increases the upwelling of the CDW onto the continental shelf and the production of the HSSW while simultaneously enhancing the polynya efficiency (Campbell et al., 2019; Gordon et al., 2007; Zhang et al., 2024). In a simulation using state-of-the-art models, Silvestri et al. (2022) showed an increase in the positive phases of the SAM in the austral summer over the 2.5–1.5 kyr BP interval (Fig. 6c) that is consistent with the transition that characterized the Edisto Inlet sea-ice regime (Fig. 6c). A shift from more prolonged and positive SAM conditions over the summer period is present throughout 2.5–1.5 kyr BP, causing more prominent mCDW intrusions over the Victoria Land coast, ultimately causing more intrusions of this water mass inside the inlet, sustaining the ice-free season (Fig. 6).

This is also consistent with the study of Mezgec et al. (2017) that compared marine and ice core records. In their study, increases in the polynya efficiency along with an increase in the katabatic wind regimes were hypothesized to start around 2.5 kyr BP, which is coeval with our record.

All these observations suggests that TEs of the benthic foraminifera in Edisto Inlet are related to the sea-ice cover variations that, ultimately, are connected to regional oceanographic and atmospheric changes, thus providing an exceptional record that offers high-resolution insight about the environmental changes over the Victoria Land coast.

4 Conclusions

In this study we analysed the Edisto Inlet by looking at the rate-of-change (RoC) of the benthic foraminiferal assemblage to infer significant environmental shifts. We showed that the RoC could bear relevant information for palaeoenvironmental reconstruction. Four different turnover events (TEs) in the benthic foraminiferal community were recognized: 3.3–3.1, 2.5–2.7, 1.2–1.0 and 0.7 kyr BP. While the first one did not have any long-term effect on the faunal composition, the other three TEs were caused by major environmental changes that had long-term effects on the faunal composition. In Edisto Inlet, changes in the RoC values are indicative of different sea-ice cover regimes. Of particular interest, the TE at 2.7–2.5 kyr BP was caused by a transition from a multi-year sea-ice-dominated environment (3.6–2.7 kyr BP) to a seasonal sea-ice-dominated one (2.5–

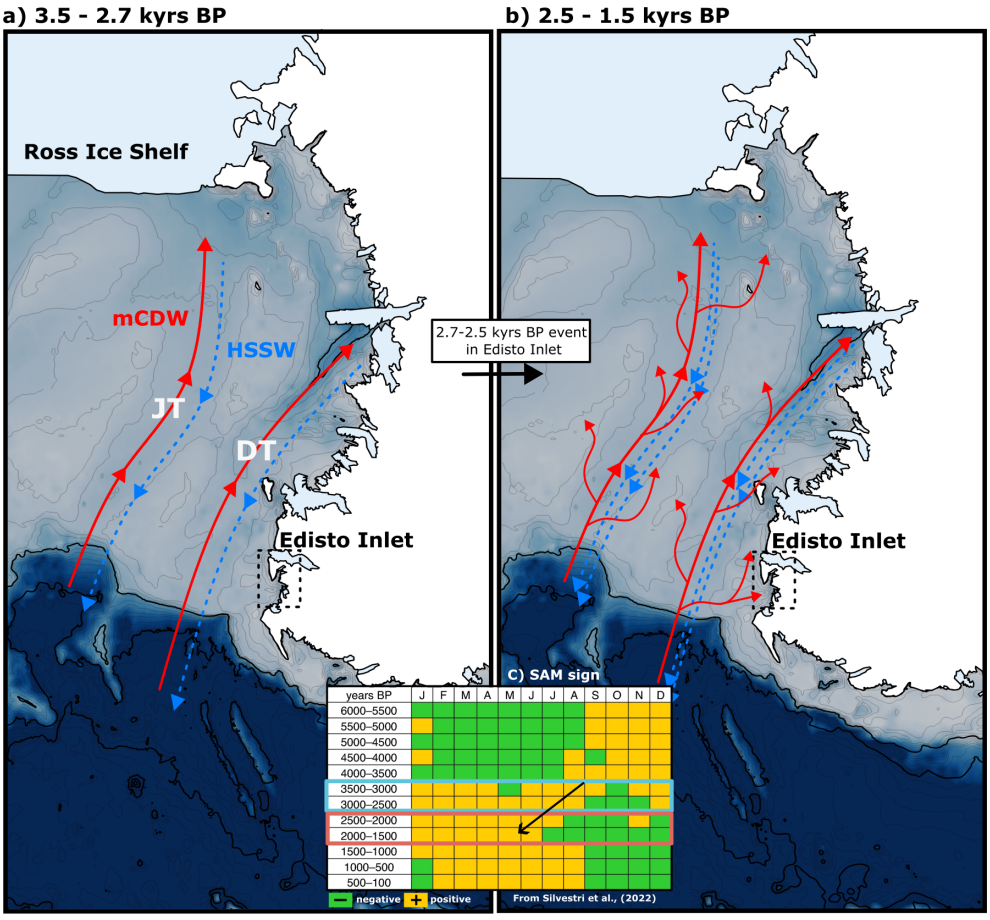

Figure 6. Conceptual regional model of the oceanographic changes in the Ross Sea over the last 3.6 kyr as identified in this study (dotted black square). Red arrows indicate the schematic flows of the superficial mCDW intrusions. Blue arrows indicate the flow of the deeper HSSW. DT: Drygalski Trough, JT: Joides Trough. **(a)** Oceanographical situation from 3.5 to 2.6 kyr BP; **(b)** oceanographic circulation from 2.5 to 1.5 kyr BP; **(c)** Southern Annular Mode values (positive in orange, negative in green) divided by month. The period covered from panel **(a)** is highlighted by the blue square in the years BP column. Panel **(b)** is highlighted by the red rectangle in the years BP column. The transition is highlighted by the black arrow. Adapted from Silvestri et al. (2022).

1.5 kyr BP). The presence of this change in the sea-ice type in the fjord had the effect of increasing the stability of the benthic community, resulting in more stable community over the seasonal sea-ice phase. The loss of *Miliammina arenacea* and *Trifarina angulosa* in conjunction with increases in *Epistominella exigua* suggest more intrusion of mCDW (modified Circumpolar Deep Water) over the 2.5–1.2 kyr BP period. XRF ratios (Zr / Rb, Br / Ti and Ca / Ti) showed a good agreement with the benthic record, demonstrating the potentiality of using RoC analysis in palaeoenvironmental studies to identify important faunal changes that are connected to environmental transitions. By looking at a more regional setting, the seasonal sea-ice phase (2.5–1.5 kyr BP) is coeval with the changes inferred over the Victoria Land coast, with a similar type of sea-ice change occurring over the same interval. The presence of positive summer phases of the Southern Annular Mode during this period strengthens this view, with more upwelling of CDW onto the shelf and increasing polynya efficiency.

Lastly, we highlight the importance that Edisto Inlet might have for studying regional oceanographical changes over the Ross Sea region, implying that the local environmental transitions that this site experiences can be used as sentinel for regional changes over the Victoria Land region. Thus, the presence of this high-resolution record could offer key insights into Holocene environmental evolution over the Ross Sea.

Data availability. All the data used in this study are included in the Supplement of this article.

Supplement. The supplement related to this article is available online at https://doi.org/10.5194/cp-21-1661-2025-supplement.

Author contributions. GG: conceptualization, formal analysis, investigation, visualization, writing the original draft and preparation; KEH: formal analysis, investigation and validation; AdR, FG and PG: data curation; AdR and KG: funding acquisition. All authors contributed to the reviewing and editing process.

Competing interests. The contact author has declared that none of the authors has any competing interests.

Disclaimer. Publisher's note: Copernicus Publications remains neutral with regard to jurisdictional claims made in the text, published maps, institutional affiliations, or any other geographical representation in this paper. While Copernicus Publications makes every effort to include appropriate place names, the final responsibility lies with the authors.

Acknowledgements. We thank the sorting centre of MNA – Trieste (Italy) for the sediment core samples and the CNR-ISMAR section of Bologna (Italy) for the XRF core scanning analysis and data. We also thank all the staff of the *Italica* and Leonardo Langone for his contributions to the sample campaign and the radiocarbon dating. Lastly, we would like to thank the anonymous reviewers and the editor for the suggestions and comments that substantially improved the article.

Financial support. This research has been supported by the Ministero dell'Università e della Ricerca (projects EDISTHO (grant no. PNRA 2018_00010) and TRACERS (grant no. PNRA2016A3/00055)).

Review statement. This paper was edited by Antje Voelker and reviewed by three anonymous referees.

References

Allen, C. S. and Weich, Z. C.: Variety and Distribution of Diatom-Based Sea Ice Proxies in Antarctic Marine Sediments of the Past 2000 Years, Geosciences (Basel), 12, 282, https://doi.org/10.3390/geosciences12080282, 2022.

Arrigo, K. R. and van Dijken, G. L.: Annual changes in sea-ice, chlorophyll a, and primary production in the Ross Sea, Antarctica, Deep-Sea Res. Pt. II, 51, 117–138, https://doi.org/10.1016/j.dsr2.2003.04.003, 2004.

Bart, P. J., DeCesare, M., Rosenheim, B. E., Majewski, W., and McGlannan, A.: A centuries-long delay between a paleo-ice-shelf collapse and grounding-line retreat in the Whales Deep Basin, eastern Ross Sea, Antarctica, Sci. Rep.-UK, 8, 12392, https://doi.org/10.1038/s41598-018-29911-8, 2018.

Battaglia, F., De Santis, L., Baradello, L., Colizza, E., Rebesco, M., Kovacevic, V., Ursella, L., Bensi, M., Accettella, D., Morelli, D., Corradi, N., Falco, P., Krauzig, N., Colleoni, F., Gordini, E., Caburlotto, A., Langone, L., and Finocchiaro, F.: The discovery of the southernmost ultra-high-resolution Holocene paleoclimate sedimentary record in Antarctica, Mar. Geol., 467, 107189, https://doi.org/10.1016/j.margeo.2023.107189, 2024.

Belt, S. T., Smik, L., Brown, T. A., Kim, J. H., Rowland, S. J., Allen, C. S., Gal, J. K., Shin, K. H., Lee, J. I., and Taylor, K. W.: Source identification and distribution reveals the potential of the geochemical Antarctic sea ice proxy IPSO25, Nat. Commun., 7, 12655, https://doi.org/10.1038/ncomms12655, 2016.

Bernhard, J. M.: Experimental and field evidence of Antarctic foraminiferal tolerance to anoxia and hydrogen sulfide, Mar. Micropaleontol., 20, 203–213, https://doi.org/10.1016/0377-8398(93)90033-T, 1993.

Budillon, G., Castagno, P., Aliani, S., Spezie, G., and Padman, L.: Thermohaline variability and Antarctic bottom water formation at the Ross Sea shelf break, Deep-Sea Res. Pt. I, 58, 1002–1018, https://doi.org/10.1016/j.dsr.2011.07.002, 2011.

Campbell, E. C., Wilson, E. A., Moore, G. W. K., Riser, S. C., Brayton, C. E., Mazloff, M. R., and Talley, L. D.: Antarctic offshore polynyas linked to Southern Hemisphere climate anomalies, Nature, 570, 319–325, https://doi.org/10.1038/s41586-019-1294-0, 2019.

Castagno, P., Falco, P., Dinniman, M. S., Spezie, G., and Budillon, G.: Temporal variability of the Circumpolar Deep Water inflow onto the Ross Sea continental shelf, J. Marine Syst., 166, 37–49, https://doi.org/10.1016/j.jmarsys.2016.05.006, 2017.

Christ, A. J., Talaia-Murray, M., Elking, N., Domack, E. W., Leventer, A., Lavoie, C., Brachfeld, S., Yoo, K. C., Gilbert, R., Jeong, S. M., Petrushak, S., Wellner, J., Balco, G., Brachfeld, S., de Batist, M., Domack, E., Gordon, A., Haran, A., Henriet, J. P., Huber, B., Ishman, S., Jeong, S., King, M., Lavoie, C., Leventer, A., McCormick, M., Mosley-Thompson, E., Pettit, E., Scambos, T., Smith, C., Thompson, L., Truffer, M., van Dover, C., Vernet, M., Wellner, J., Yu, K., and Zagorodnov, V.: Late Holocene glacial advance and ice shelf growth in Barilari Bay, Graham Land, West Antarctic Peninsula, Bull. Geol. Soc. Am., 127, 297–315, https://doi.org/10.1130/B31035.1, 2015.

Croudace, I. and Rothwell, R. G. (Eds.): Micro-XRF Studies of Sediment Cores, Springer Netherlands, Dordrecht, https://doi.org/10.1007/978-94-017-9849-5, 2015.

Dale, E. R., McDonald, A. J., Coggins, J. H. J., and Rack, W.: Atmospheric forcing of sea ice anomalies in the Ross Sea polynya region, The Cryosphere, 11, 267–280, https://doi.org/10.5194/tc-11-267-2017, 2017.

Dinniman, M. S., Klinck, J. M., and Smith, W. O.: A model study of Circumpolar Deep Water on the West Antarctic Peninsula and Ross Sea continental shelves, Deep-Sea Res. Pt. II, 58, 1508–1523, https://doi.org/10.1016/j.dsr2.2010.11.013, 2011.

Di Roberto, A., Re, G., Scateni, B., Petrelli, M., Tesi, T., Capotondi, L., Morigi, C., Galli, G., Colizza, E., Melis, R., Torricella, F., Giordano, P., Giglio, F., Gallerani, A., and Gariboldi, K.: Cryptotephras in the marine sediment record of the Edisto Inlet, Ross Sea: Implications for the volcanology and tephrochronology of northern Victoria Land, Antarctica, Quaternary Science Advances, 10, https://doi.org/10.1016/j.qsa.2023.100079, 2023.

Drucker, R., Martin, S., and Kwok, R.: Sea ice production and export from coastal polynyas in the Weddell and Ross Seas, Geophys. Res. Lett., 38, https://doi.org/10.1029/2011gl048668, 2011.

Duffield, C. J., Hess, S., Norling, K., and Alve, E.: The response of Nonionella iridea and other benthic

foraminifera to "fresh" organic matter enrichment and physical disturbance, Mar. Micropaleontol., 120, 20–30, https://doi.org/10.1016/j.marmicro.2015.08.002, 2015.

Emslie, S. D., Berkman, P. A., Ainley, D. G., Coats, L., and Polito, M.: Late-Holocene initiation of ice-free ecosystems in the southern Ross Sea, Antarctica, Mar. Ecol. Prog. Ser., 262, 19–25, https://doi.org/10.3354/meps262019, 2003.

Emslie, S. D., McKenzie, A., and Patterson, W. P.: The rise and fall of an ancient adélie penguin 'supercolony' at cape adare, antarctica, Roy. Soc. Open Sci., 5, https://doi.org/10.1098/rsos.172032, 2018.

Finocchiaro, F., Langone, L., Colizza, E., Fontolan, G., Giglio, F., and Tuzzi, E.: Record of the early Holocene warming in a laminated sediment core from Cape Hallett Bay (Northern Victoria Land, Antarctica), Global Planet. Change, 45, 193–206, https://doi.org/10.1016/j.gloplacha.2004.09.003, 2005.

Fogt, R. L. and Marshall, G. J.: The Southern Annular Mode: Variability, trends, and climate impacts across the Southern Hemisphere, WIREs Climate Change, 11, e652, https://doi.org/10.1002/wcc.652, 2020.

Foster, D. R., KSchoonmaker, P., and Pickett, S. T. A.: Insights from paleoecology to community ecology, Trends Ecol. Evol., 5, 119–122, https://doi.org/10.1016/0169-5347(90)90166-B, 1990.

Fraser, A. D., Wongpan, P., Langhorne, P. J., Klekociuk, A. R., Kusahara, K., Lannuzel, D., Massom, R. A., Meiners, K. M., Swadling, K. M., Atwater, D. P., Brett, G. M., Corkill, M., Dalman, L. A., Fiddes, S., Granata, A., Guglielmo, L., Heil, P., Leonard, G. H., Mahoney, A. R., McMinn, A., van der Merwe, P., Weldrick, C. K., and Wienecke, B.: Antarctic Landfast Sea Ice: A Review of Its Physics, Biogeochemistry and Ecology, https://doi.org/10.1029/2022RG000770, 2023.

Galli, G., Morigi, C., Melis, R., Di Roberto, A., Tesi, T., Torricella, F., Langone, L., Giordano, P., Colizza, E., Capotondi, L., Gallerani, A., and Gariboldi, K.: Paleoenvironmental changes related to the variations of the sea-ice cover during the Late Holocene in an Antarctic fjord (Edisto Inlet, Ross Sea) inferred by foraminiferal association, J. Micropalaeontol., 42, 95–115, https://doi.org/10.5194/jm-42-95-2023, 2023.

Galli, G., Morigi, C., Thuy, B., and Gariboldi, K.: Late Holocene echinoderm assemblages can serve as paleoenvironmental tracers in an Antarctic fjord, Sci. Rep.-UK, 14, https://doi.org/10.1038/s41598-024-66151-5, 2024.

Gordon, A. L., Visbeck, M., and Comiso, J. C.: A Possible Link between the Weddell Polynya and the Southern Annular Mode, J. Climate, 20, 2558–2571, https://doi.org/10.1175/JCLI4046.1, 2007.

Hall, B. L., Hoelzel, A. R., Baroni, C., Denton, G. H., Le Boeuf, B. J., Overturf, B., and Topf, A. L.: Holocene elephant seal distribution implies warmer-than-present climate in the Ross Sea, P. Natl. Acad. Sci. USA, 103, 10213–10217, https://doi.org/10.1073/pnas.0604002103, 2006.

Hall, B. L., Koch, P. L., Baroni, C., Salvatore, M. C., Hoelzel, A. R., de Bruyn, M., and Welch, A. J.: Widespread southern elephant seal occupation of the Victoria land coast implies a warmer-than-present Ross Sea in the mid-to-late Holocene, Quaternary Sci. Rev., 303, https://doi.org/10.1016/j.quascirev.2023.107991, 2023.

Hansen, K. E., Pearce, C., and Seidenkrantz, M. S.: Response of Arctic benthic foraminiferal traits to past environmental changes, Sci. Rep.-UK, 13, https://doi.org/10.1038/s41598-023-47603-w, 2023.

Harloff, J. and Mackensen, A.: Recent benthic foraminiferal associations and ecology of the Scotia Sea and Argentin Basin, Mar. Micropaleontol., 31, 1–29, https://doi.org/10.1016/S0377-8398(96)00059-X, 1997.

Herguera, J. C. and Berger, W. H.: Paleoproductivity from benthic foraminifera abundance: Glacial to postglacial change in the west-equatorial Pacific, Geology, 19, 1173–1176, https://doi.org/10.1130/0091-7613(1991)019<1173:PFBFAG>2.3.CO;2, 1991.

Howe, J. A., Austin, W. E. N., Forwick, M., Paetzel, M., Harland, R., and Cage, A. G.: Fjord systems and archives: a review, Geol. Soc. Spec. Publ., 344, 5–15, https://doi.org/10.1144/sp344.2, 2010.

Ishman, S. E. and Sperling, M. R.: Benthic foraminiferal record of Holocene deep-water evolution in the Palmer Deep, western Antarctica Peninsula, Geology, 30, 435–438, https://doi.org/10.1130/0091-7613(2002)030<0435:BFROHD>2.0.CO;2, 2002.

Ishman, S. E. and Szymcek, P.: Foraminiferal Distributions in the Former Larsen-A Ice Shelf and Prince Gustav Channel Region, Eastern Antarctic Peninsula Margin: A Baseline for Holocene Paleoenvironmental Change, in: Antarctic Peninsula Climate Variability: Historical and Paleoenvironmental Perspectives, 239–260, https://doi.org/10.1029/AR079p0239, 2003.

Jacobson, G. L. and Grimm, E. C.: A Numerical Analysis of Holocene Forest and Prairie Vegetation in Central Minnesota, Ecology, 67, 958–966, https://doi.org/10.2307/1939818, 1986.

Knudsen, K. L., Stabell, B., Seidenkrantz, M.-S., EirÍKsson, J. Ó. N., and Blake, W.: Deglacial and Holocene conditions in northernmost Baffin Bay: sediments, foraminifera, diatoms and stable isotopes, Boreas, 37, 346–376, https://doi.org/10.1111/j.1502-3885.2008.00035.x, 2008.

Kyrmanidou, A., Vadman, K. J., Ishman, S. E., Leventer, A., Brachfeld, S., Domack, E. W., and Wellner, J. S.: Late Holocene oceanographic and climatic variability recorded by the Perseverance Drift, northwestern Weddell Sea, based on benthic foraminifera and diatoms, Mar. Micropaleontol., 141, 10–22, https://doi.org/10.1016/j.marmicro.2018.03.001, 2018.

Lamy, F., Winckler, G., Arz, H. W., Farmer, J. R., Gottschalk, J., Lembke-Jene, L., Middleton, J. L., van der Does, M., Tiedemann, R., Alvarez Zarikian, C., Basak, C., Brombacher, A., Dumm, L., Esper, O. M., Herbert, L. C., Iwasaki, S., Kreps, G., Lawson, V. J., Lo, L., Malinverno, E., Martinez-Garcia, A., Michel, E., Moretti, S., Moy, C. M., Ravelo, A. C., Riesselman, C. R., Saavedra-Pellitero, M., Sadatzki, H., Seo, I., Singh, R. K., Smith, R. A., Souza, A. L., Stoner, J. S., Toyos, M., de Oliveira, I. M. V. P., Wan, S., Wu, S., and Zhao, X.: Five million years of Antarctic Circumpolar Current strength variability, Nature, 627, 789–796, https://doi.org/10.1038/s41586-024-07143-3, 2024.

Leventer, A., Dunbar, R. B., and DeMaster, D. J.: Diatom evidence for Late Holocene climatic events in Granite Harbor, Antarctica, Paleoceanography, 8, 373–386, https://doi.org/10.1029/93PA00561, 1993.

Li, B., Yoon, H., and Park, B.: Foraminiferal assemblages and $CaCO_3$ dissolution since the last deglaciation in the Maxwell Bay, King George Island, Antarctica, Mar. Geol., 169, 239–257, https://doi.org/10.1016/S0025-3227(00)00059-1, 2000.

Lüning, S., Gałka, M., and Vahrenholt, F.: The Medieval Climate Anomaly in Antarctica, Palaeogeogr. Palaeocl., 532, https://doi.org/10.1016/j.palaeo.2019.109251, 2019.

Majewski, W.: Benthic foraminiferal communities: distribution and ecology in Admiralty Bay, King George Island, West Antarctica, Pol. Polar Res., 26, 159–214, 2005.

Majewski, W.: Benthic foraminifera from West Antarctic fiord environments: An overview, Pol. Polar Res., 31, 61–82, https://doi.org/10.4202/ppres.2010.05, 2010.

Majewski, W. and Anderson, J. B.: Holocene foraminiferal assemblages from Firth of Tay, Antarctic Peninsula: Paleoclimate implications, Mar. Micropaleontol., 73, 135–147, https://doi.org/10.1016/j.marmicro.2009.08.003, 2009.

Majewski, W., Prothro, L. O., Simkins, L. M., Demianiuk, E. J., and Anderson, J. B.: Foraminiferal Patterns in Deglacial Sediment in the Western Ross Sea, Antarctica: Life Near Grounding Lines, 35, e2019PA003716, https://doi.org/10.1029/2019PA003716, 2020.

Majewski, W., Wellner, J. S., and Anderson, J. B.: Environmental connotations of benthic foraminiferal assemblages from coastal West Antarctica, Mar. Micropaleontol., 124, 1–15, https://doi.org/10.1016/j.marmicro.2016.01.002, 2016.

Majewski, W., Bart, P. J., and McGlannan, A. J.: Foraminiferal assemblages from ice-proximal paleo-settings in the Whales Deep Basin, eastern Ross Sea, Antarctica, Palaeogeogr. Palaeocl., 493, 64–81, https://doi.org/10.1016/j.palaeo.2017.12.041, 2018.

Majewski, W., Szczuciński, W., and Gooday, A. J.: Unique benthic foraminiferal communities (stained) in diverse environments of sub-Antarctic fjords, South Georgia, Biogeosciences, 20, 523–544, https://doi.org/10.5194/bg-20-523-2023, 2023.

Marshall, G. J.: Trends in the Southern Annular Mode from observations and reanalyses, J. Climate, 16, 4134–4143, https://doi.org/10.1175/1520-0442(2003)016<4134:TITSAM>2.0.CO;2, 2003.

Massé, G., Belt, S. T., Crosta, X., Schmidt, S., Snape, I., Thomas, D. N., and Rowland, S. J.: Highly branched isoprenoids as proxies for variable sea ice conditions in the Southern Ocean, Antarct. Sci., 23, 487–498, https://doi.org/10.1017/s0954102011000381, 2011.

Mathiot, P., Jourdain, N. C., Barnier, B., Gallée, H., Molines, J. M., Le Sommer, J., and Penduff, T.: Sensitivity of coastal polynyas and high-salinity shelf water production in the Ross Sea, Antarctica, to the atmospheric forcing, Ocean Dynam., 62, 701–723, https://doi.org/10.1007/s10236-012-0531-y, 2012.

Matsuoka, K., Skoglund, A., Roth, G., de Pomereu, J., Griffiths, H., Headland, R., Herried, B., Katsumata, K., Le Brocq, A., Licht, K., Morgan, F., Neff, P. D., Ritz, C., Scheinert, M., Tamura, T., Van de Putte, A., van den Broeke, M., von Deschwanden, A., Deschamps-Berger, C., Van Liefferinge, B., Tronstad, S., and Melvær, Y.: Quantarctica, an integrated mapping environment for Antarctica, the Southern Ocean, and sub-Antarctic islands, Environ. Modell. Softw., 140, https://doi.org/10.1016/j.envsoft.2021.105015, 2021.

Melis, R. and Salvi, G.: Late Quaternary foraminiferal assemblages from western Ross Sea (Antarctica) in relation to the main glacial and marine lithofacies, Mar. Micropaleontol., 70, 39–53, https://doi.org/10.1016/j.marmicro.2008.10.003, 2009.

Melis, R., Capotondi, L., Torricella, F., Ferretti, P., Geniram, A., Hong, J. K., Kuhn, G., Khim, B.-K., Kim, S., Malinverno, E., Yoo, K. C., and Colizza, E.: Last Glacial Maximum to Holocene paleoceanography of the northwestern Ross Sea inferred from sediment core geochemistry and micropaleontology at Hallett Ridge, J. Micropalaeontol., 40, 15–35, https://doi.org/10.5194/jm-40-15-2021, 2021.

Mezgec, K., Stenni, B., Crosta, X., Masson-Delmotte, V., Baroni, C., Braida, M., Ciardini, V., Colizza, E., Melis, R., Salvatore, M. C., Severi, M., Scarchilli, C., Traversi, R., Udisti, R., and Frezzotti, M.: Holocene sea ice variability driven by wind and polynya efficiency in the Ross Sea, Nat. Commun., 8, 1334, https://doi.org/10.1038/s41467-017-01455-x, 2017.

Mottl, O., Flantua, S. G. A., Bhatta, K. P., Felde, V. A., Giesecke, T., Goring, S., Grimm, E. C., Haberle, S., Hooghiemstra, H., Ivory, S., Kuneš, P., Wolters, S., Seddon, A. W. R., and Williams, J. W.: Global acceleration in rates of vegetation change over the past 18 000 years, Science, 372, 860–864, https://doi.org/10.1126/science.abg1685, 2021a.

Mottl, O., Grytnes, J. A., Seddon, A. W. R., Steinbauer, M. J., Bhatta, K. P., Felde, V. A., Flantua, S. G. A., and Birks, H. J. B.: Rate-of-change analysis in paleoecology revisited: A new approach, Rev. Palaeobot. Palyno., 293, https://doi.org/10.1016/j.revpalbo.2021.104483, 2021b.

Murray, J. W.: Ecology and palaeoecology of benthic foraminifera, Routledge, https://doi.org/10.4324/9781315846101, 1991.

Murray, J. W.: Ecology and Applications of Benthic Foraminifera, Cambridge University Press, https://doi.org/10.1017/CBO9780511535529, 2006.

Murray, J. W. and Pudsey, C. J.: Living (stained) and dead foraminifera from the newly ice-free Larsen Ice Shelf, Weddell Sea, Antarctica: Ecology and taphonomy, Mar. Micropaleontol., 53, 67–81, https://doi.org/10.1016/j.marmicro.2004.04.001, 2004.

Orsi, A. H. and Wiederwohl, C. L.: A recount of Ross Sea waters, Deep-Sea Res. Pt. II, 56, 778–795, https://doi.org/10.1016/j.dsr2.2008.10.033, 2009.

O'Sullivan, J. D., Terry, J. C. D., and Rossberg, A. G.: Intrinsic ecological dynamics drive biodiversity turnover in model metacommunities, Nat. Commun., 12, https://doi.org/10.1038/s41467-021-23769-7, 2021.

Pan, B. J., Vernet, M., Manck, L., Forsch, K., Ekern, L., Mascioni, M., Barbeau, K. A., Almandoz, G. O., and Orona, A. J.: Environmental drivers of phytoplankton taxonomic composition in an Antarctic fjord, Prog. Oceanogr., 183, https://doi.org/10.1016/j.pocean.2020.102295, 2020.

Peck, V. L., Allen, C. S., Kender, S., McClymont, E. L., and Hodgson, D. A.: Oceanographic variability on the West Antarctic Peninsula during the Holocene and the influence of upper circumpolar deep water, Quaternary Sci. Rev., 119, 54–65, https://doi.org/10.1016/j.quascirev.2015.04.002, 2015.

Piva, A., Asioli, A., Schneider, R. R., Trincardi, F., Andersen, N., Colmenero-Hidalgo, E., Dennielou, B., Flores, J. A., and Vigliotti, L.: Climatic cycles as expressed in sediments of the PROMESSI borehole PRAD1-2, central Adriatic, for the last 370 ka: 1. Integrated stratigraphy, Geochem. Geophy. Geosy., 9, https://doi.org/10.1029/2007GC001713, 2008.

R Core Team: A Language and Environment for Statistical Computing, R Foundation for Statistical Computing, Vienna, Austria, https://www.R-project.org/ (last access: 15 September 2020), 2023.

Reeh, N., Mayer, C., Miller, H., Thomsen, H. H., and Weidick, A.: Present and past climate control on fjord glaciations in Greenland: Implications for IRD-deposition in the sea, Geophys. Res. Lett., 26, 1039–1042, https://doi.org/10.1029/1999GL900065, 1999.

Rusciano, E., Budillon, G., Fusco, G., and Spezie, G.: Evidence of atmosphere–sea ice–ocean coupling in the Terra Nova Bay polynya (Ross Sea – Antarctica), Cont. Shelf Res., 61–62, 112–124, https://doi.org/10.1016/j.csr.2013.04.002, 2013.

Sabbatini, A., Morigi, C., Ravaioli, M., and Negri, A.: Abyssal benthic foraminifera in the Polar Front region (Pacific sector): Faunal composition, standing stock and size structure, Chem. Ecol., 20, S117–S129, https://doi.org/10.1080/02757540410001655387, 2004.

Seidenkrantz, M.-S.: Benthic foraminifera as palaeo sea-ice indicators in the subarctic realm – examples from the Labrador Sea–Baffin Bay region, Quaternary Sci. Rev., 79, 135–144, https://doi.org/10.1016/j.quascirev.2013.03.014, 2013.

Seidenstein, J. L., Cronin, T. M., Gemery, L., Keigwin, L. D., Pearce, C., Jakobsson, M., Coxall, H. K., Wei, E. A., and Driscoll, N. W.: Late Holocene paleoceanography in the Chukchi and Beaufort Seas, Arctic Ocean, based on benthic foraminifera and ostracodes, arktos, 4, 1–17, https://doi.org/10.1007/s41063-018-0058-7, 2018.

Sen Gupta, B. K.: Modern Foraminifera, Springer Netherlands, Dordrecht, https://doi.org/10.1007/0-306-48104-9, 2003.

Shimadzu, H., Dornelas, M., and Magurran, A. E.: Measuring temporal turnover in ecological communities, Methods Ecol. Evol., 6, 1384–1394, https://doi.org/10.1111/2041-210X.12438, 2015.

Silvestri, G., Berman, A. L., Braconnot, P., and Marti, O.: Long-term trends in the Southern Annular Mode from transient Mid- to Late Holocene simulation with the IPSL-CM5A2 climate model, Clim. Dynam., 59, 903–914, https://doi.org/10.1007/s00382-022-06160-0, 2022.

Simpson, G. L.: Modelling palaeoecological time series using generalised additive models, Front. Ecol. Evol., 6, https://doi.org/10.3389/fevo.2018.00149, 2018.

Smith Jr., W. O., Ainley, D. G., Arrigo, K. R., and Dinniman, M. S.: The oceanography and ecology of the Ross Sea, Annu. Rev. Mar. Sci., 6, 469–487, https://doi.org/10.1146/annurev-marine-010213-135114, 2014.

Smith, W., Sedwick, P., Arrigo, K., Ainley, D., and Orsi, A.: The Ross Sea in a Sea of Change, Oceanography, 25, 90–103, https://doi.org/10.5670/oceanog.2012.80, 2012.

Smith, W. O. and Gordon, L. I.: Hyperproductivity of the Ross Sea (Antarctica) polynya during austral spring, Geophys. Res. Lett., 24, 233–236, https://doi.org/10.1029/96gl03926, 1997.

Stenni, B., Curran, M. A. J., Abram, N. J., Orsi, A., Goursaud, S., Masson-Delmotte, V., Neukom, R., Goosse, H., Divine, D., van Ommen, T., Steig, E. J., Dixon, D. A., Thomas, E. R., Bertler, N. A. N., Isaksson, E., Ekaykin, A., Werner, M., and Frezzotti, M.: Antarctic climate variability on regional and continental scales over the last 2000 years, Clim. Past, 13, 1609–1634, https://doi.org/10.5194/cp-13-1609-2017, 2017.

Strugnell, J. M., McGregor, H. V., Wilson, N. G., Meredith, K. T., Chown, S. L., Lau, S. C. Y., Robinson, S. A., and Saunders, K. M.: Emerging biological archives can reveal ecological and climatic change in Antarctica, Global Change Biology, 28, https://doi.org/10.1111/gcb.16356, 2022.

Taylor, S. P., Patterson, M. O., Lam, A. R., Jones, H., Woodard, S. C., Habicht, M. H., Thomas, E. K., and Grant, G. R.: Expanded North Pacific Subtropical Gyre and Heterodyne Expression During the Mid-Pleistocene, Paleoceanogr. Paleoclimatol., 37, https://doi.org/10.1029/2021PA004395, 2022.

Tesi, T., Belt, S. T., Gariboldi, K., Muschitiello, F., Smik, L., Finocchiaro, F., Giglio, F., Colizza, E., Gazzurra, G., Giordano, P., Morigi, C., Capotondi, L., Nogarotto, A., Köseoğlu, D., Di Roberto, A., Gallerani, A., and Langone, L.: Resolving sea ice dynamics in the north-western Ross Sea during the last 2.6 ka: From seasonal to millennial timescales, Quaternary Sci. Rev., 237, https://doi.org/10.1016/j.quascirev.2020.106299, 2020.

Tomašových, A. and Kidwell, S. M.: The effects of temporal resolution on species turnover and on testing metacommunity models, Am. Nat., 175, 587–606, https://doi.org/10.1086/651661, 2010.

Toyos, M. H., Lamy, F., Lange, C. B., Lembke-Jene, L., Saavedra-Pellitero, M., Esper, O., and Arz, H. W.: Antarctic Circumpolar Current Dynamics at the Pacific Entrance to the Drake Passage Over the Past 1.3 Million Years, Paleoceanogr. Paleoclimatol., 35, https://doi.org/10.1029/2019pa003773, 2020.

Wang, Y., Zhou, M., Zhang, Z., and Dinniman, M. S.: Seasonal variations in Circumpolar Deep Water intrusions into the Ross Sea continental shelf, Front. Mar. Sci., 10, https://doi.org/10.3389/fmars.2023.1020791, 2023.

Waters, R. L., van den Enden, R., and Marchant, H. J.: Summer microbial ecology off East Antarctica (80–150° E): protistan community structure and bacterial abundance, Deep-Sea Res. Pt. II, 47, 2401–2435, https://doi.org/10.1016/S0967-0645(00)00030-8, 2000.

Whitworth, T. and Orsi, A. H.: Antarctic Bottom Water production and export by tides in the Ross Sea, Geophys. Res. Lett., 33, https://doi.org/10.1029/2006gl026357, 2006.

Wongpan, P., Meiners, K. M., Vancoppenolle, M., Fraser, A. D., Moreau, S., Saenz, B. T., Swadling, K. M., and Lannuzel, D.: Gross Primary Production of Antarctic Landfast Sea Ice: A Model-Based Estimate, J. Geophys. Res.-Oceans, 129, https://doi.org/10.1029/2024JC021348, 2024.

Wood, S.: mgcv: GAMs and generalized ridfe regression for R, R news, 1, 20–25, 2001.

Wu, L., Wang, R., Krijgsman, W., Chen, Z., Xiao, W., Ge, S., and Wu, J.: Deciphering Color Reflectance Data of a 520 kyr Sediment Core From the Southern Ocean: Method Application and Paleoenvironmental Implications, Geochem. Geophy. Geosy., 20, 2808–2826, https://doi.org/10.1029/2019GC008212, 2019.

Wu, L., Wilson, D. J., Wang, R., Yin, X., Chen, Z., Xiao, W., and Huang, M.: Evaluating Zr/Rb Ratio From XRF Scanning as an Indicator of Grain-Size Variations of Glaciomarine Sediments in the Southern Ocean, Geochem. Geophy. Geosy., 21, https://doi.org/10.1029/2020GC009350, 2020.

Xu, Q. B., Yang, L. J., Gao, Y. S., Sun, L. G., and Xie, Z. Q.: 6,000-Year Reconstruction of Modified Circumpolar Deep Water Intrusion and Its Effects on Sea Ice and Penguin in the Ross Sea, Geophys. Res. Lett., 48, https://doi.org/10.1029/2021GL094545, 2021.

Yokoyama, Y., Anderson, J. B., Yamane, M., Simkins, L. M., Miyairi, Y., Yamazaki, T., Koizumi, M., Suga, H., Kusahara, K., Prothro, L., Hasumi, H., Southon, J. R., and Ohkouchi, N.: Widespread collapse of the Ross Ice Shelf during the

late Holocene, P. Natl. Acad. Sci. USA, 113, 2354–2359, https://doi.org/10.1073/pnas.1516908113, 2016.

Zhang, Z., Xie, C., Castagno, P., England, M. H., Wang, X., Dinniman, M. S., Silvano, A., Wang, C., Zhou, L., Li, X., Zhou, M., and Budillon, G.: Evidence for large-scale climate forcing of dense shelf water variability in the Ross Sea, Nat. Commun., 15, 8190, https://doi.org/10.1038/s41467-024-52524-x, 2024.

Zhou, Y., McManus, J. F., Jacobel, A. W., Costa, K. M., Wang, S., and Alvarez Caraveo, B.: Enhanced iceberg discharge in the western North Atlantic during all Heinrich events of the last glaciation, Earth Planet. Sc. Lett., 564, https://doi.org/10.1016/j.epsl.2021.116910, 2021.

Ziegler, M., Jilbert, T., De Lange, G. J., Lourens, L. J., and Reichart, G. J.: Bromine counts from XRF scanning as an estimate of the marine organic carbon content of sediment cores, Geochem. Geophy. Geosy., 9, https://doi.org/10.1029/2007GC001932, 2008.